PERFORMANCE SIMULATIONS OF A 72-CELL, A-SI HET MODULE WITH DIFFERENT TAB-INTERCONNECTION GEOMETRIES

Julien Eymard, Benjamin Commault, Félix Gerenton, Raphaël Clerc, Mathieu Hébert

PERFORMANCE SIMULATIONS OF A 72-CELL, A-SI HET MODULE WITH DIFFERENT TAB-INTERCONNECTION GEOMETRIES

Julien Eymard[1], Benjamin Commault[1], Felix Gerenton[1], Thomas Guérin[1], Raphael Clerc[2], Mathieu Hebert[2]

1 - Univ. Grenoble Alpes, CEA, LITEN, INES, LMPV, F-38000 Grenoble, France
2 - Univ Lyon, UJM-Saint-Etienne, CNRS, Institut d Optique Graduate School, Laboratoire Hubert Curien UMR 5516, F-42023, SAINT-ETIENNE, France

ABSTRACT: The use of half-cells is known to be an effective way to increase cell-to-module (CTM) ratio, thanks to lower resistive losses. Multi-wire interconnection allows reducing silver paste consumption; offering better effective shading compared to flat ribbons. The number and the diameter of wires influence the series resistance and photo-generated current values in opposite ways, leading to an optimal value in CTM. In this paper, the impact of grid resistance and effective shading of wires on the optimum number and diameter of wires is evaluated. Two module architectures are considered, half- and full-cells. Decreasing grid resistance by a factor two, even if it allows using fewer wires, has only a small impact on CTM gain (+ 0.3 %). A large range of possible values of effective shading is found in the literature. The sensitivity analysis shows that it has a major impact on CTM (± 1.3 %), at constant consumption in amount of wires. The use of half-cells allows to employ less wires with a smaller diameter than in full-cell modules. It is a double gain, in CTM performance (+ 2.2 %) and in consumption of raw material (- 40 %).

Keywords: cell-to-module ratio, CTM, multi-wire, half-cell, effective shading; optimization;

1 INTRODUCTION

The photovoltaic (PV) solar energy industry has grown with an average of + 50% per year in the last years. In order to strengthen their position in the market, PV companies seek cost reductions and an increase of technical performance. A standard photovoltaic module is composed of photovoltaic cells electrically connected by ribbons and encapsulated in polymers and glass. Cell-to-module (CTM) analysis is useful to quantify losses and gains in the module. It related the performance of the module with the performance of the cells composing the module, in order to identify opportunities for improvement. In this work, the CTM classification proposed by Haedrich *et al.* [1] is used as it includes optical effects: reflection, absorption, shading and cell / module coupling, and electrical losses like resistance and mismatch.

Reduction of power losses by optimization of the PV module manufacturing process is a way to reduce costs. A popular way is cutting cells into two half parts. The result is a current two times lower, thus dividing resistive power losses in the module by a factor four. Another way that may induce lower power losses is larger wires diameter. This latter results in higher cell shading but smaller series resistance. Increasing the number of wires has both previous effects, but also decreases the finger resistance of the solar cell [2]. Thus, it exists a compromise resulting in an optimum in the number and diameter of the wires. Such optimization is a common approach [3]. The purpose of this work is to analyse the variation of this optimum when varying the effective shading of wires and the grid resistance. A specific case is here presented, a monofacial PV module with 72 heterojunction (HJT) Si-solar full- and half-cells with a multi-wire interconnection.

First, we present modelling considerations about the electrical resistance of the wires and their shading impact on cells. Second, parameters of this case are characterized and explained, such as the effective diameter and line resistance. Third, results of the optimization in terms of number and diameter of wires are detailed. To conclude, a sensitivity analysis on the optimum of effective shading and grid resistance is presented.

2 MODELLING CONSIDERATIONS

2.1 Modelling of the solar cell and module

The 72 full-cells are supposed to be identical and described by a single diode model with five parameters: the photo generated current I_{ph_c}, the diode saturation current I_{0_c}, the ideality factor of the dioden_{id_c}, the series resistance of the cell without finger contribution R_{s_c} and the shunt resistance R_{sh_c}. The current I and voltage V are thus given by the following equation:

$$I = I_{ph_c} - I_{0_c}\left(e^{\frac{V+IR_{s_c}}{n_{id_c}V_{th}}} - 1\right) - \frac{V + IR_{s_c}}{R_{sh_c}}$$

The parameters are extracted from curve fitting of the IV characteristics of each cells. The mean values of the parameters are given in Table I. The half-cell case is supposed to be an ideal case: no additional losses occur at the cutting step. In the half-cell case, the photo-generated current I_{ph_c} and the diode saturation current I_{0_c} are divided by a factor two, whereas the series resistance R_{s_c} and the shunt resistance R_{sh_c} are multiplied by a factor two.

Table I: Mean of the five parameters of the single diode model used in simulation for the full-cell case

$I_{ph_c}(A)$	$I_{0_c}(nA)$	n_{id_n}	$R_{s_c}(m\Omega)$	$R_{sh_c}(\Omega)$
9.187	0.7607	1.234	3.999	2.417

When the 72 full-cells or 144 half-cells are connected in series and encapsulated to make the module, only the photo-generated current $I_{ph_{cell}}$ and the series resistance R_{s_c} are affected. The three other parameters I_{0_c}, n_{id_c} and R_{sh_c} are kept constant.

2.2 Change in photo-generated current I_{ph} from cell to module

Several effects due to module architecture can reduce or increase the photo-generated current of the solar cell

measured in air:

- Reflection and absorption in glass and encapsulant, shading of interconnection ribbons, cause losses in incident flux
- Cell coupling (index matching between cell and encapsulant), glass/air interface coupling with fingers, wires and backsheet causes additional gains compared to the non-encapsulated case

Varying the number and diameter of the wires mainly affects: (i) the shading of the solar cell, (ii) the coupling between wires and glass/air interface. The wire shading is defined as the ratio of the projected wire area on the solar cell area. The shading ratio k_s is defined as the area of the wire n_w with a diameter d_w and a length on the cell L_w on the cell area A_c, corrected by the area of the finger laying under the wires:

$$k_s = d_w\, n_w \left(L_w - n_f l_f\right) \frac{1}{A_c}$$

Coupling between glass and wires is explained by the reflection to the cell of a certain percent of the incoming light falling on wires [4]. This results in an effective shading diameter of wire smaller than the physical diameter. Shading of wires and coupling between glass and wire affect the intensities of light reaching the solar cell, and thus directly affect the photo-generated current. The photo-generated current of the module I_{ph_m} is thus linked to the photo-generated current of the cell I_{ph_c} by the following equation, where k_{stack} represent the change in I_{ph} which is independent of the number and diameter of the wires:

$$I_{ph_{module}} = I_{ph_c}(1 - k_s)\, k_{stack}$$

The value k_{stack} encompasses losses effects like absorption and reflection by the optical layers, but also gain effects like index matching between cell and encapsulant, coupling of fingers with glass/air interface and coupling of cell and backsheet. Thus, the factor k_{stack} can be smaller or greater than one.

2.3 Additional series resistance R_s from cell to module

The cells used are busbar-less and have been measured with GridTouch method [5]. The additional series resistance of the module is the sum of the contributions of fingers R_{s_f}, wires R_{s_w} and string ribbons R_{s_r}. These parameters depend on the number of wires n_w:

$$R_{s_m} = R_{s_c} + R_{s_f} + R_{s_w} + R_{s_r}$$

The finger contribution in the series resistance of the module is proportional to the grid resistance $R_{s_{grid}}$, to the number of cell n_c, and inversely proportional to the square of the number of wires n_w. Both contributions of the front and back side must be added. :

$$R_{s_f} = \frac{R_{s_{grid}}}{12\, n_w^2}\, n_c$$

The wire contribution can be divided in two parts: one due to length of the wire on the solar cell $R_{s_{wc}}$ and one due to distance d_{ic} between cells:

$$R_{s_{wc}} = \frac{4\,\rho_w}{\pi\, d_w^2\, n_w}\left(\frac{2L_w\, n_c}{3} + d_{ic}\, n_s\, (n_{c_s} + 1)\right)$$

3 CHARACTERIZATION OF THE INPUT PARAMETERS OF THE MODEL

In this part, the method is detailed and results of the measurement for the parameters of the case model are presented.

3.1 Characterization of line resistance of wires

The line resistance of the wire is characterized with the transmission line measurement method. A ramp of voltage is applied to two wires at selected distances between them. At a particular distance, applying a voltage ramp and measuring the slope of the IV curve gives the resistance between the wires. Repeating the procedure at various distances between voltage probes leads to a linear relation. The line resistance is the slope of the curve; the contact resistance is the value for a zero distance (Figure 2):

$$R_{line} = 3.419 \pm 0.003\ m\Omega/cm$$

The wire resistivity can be deduced from this value and the line resistance of other wire diameters can be inferred: $\rho_w = 1.81 \pm 0.02\ 10^{-8}\ \Omega.m$. Similarly, the line resistance of the string interconnection ribbons is $R_{s_{line}} = 0.12\ m\Omega/cm$.

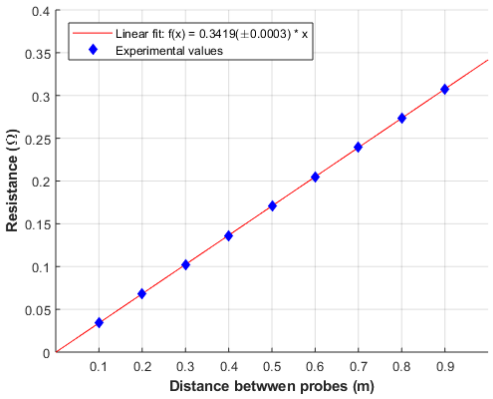

Figure 2: Measurement of the line resistance R_{line_w}. The results show a linear relation, with a relative error on the value around 0.1%. The contact resistance between probes and wire is negligible (smaller than $2.10^{-5}\ \Omega$).

The grid resistance can be characterized with a similar method. A foil of 18 wires, with wire interspacing of $l_w = 8.1\ mm$, is applied on the front side, with wires extending on both sides of the module, as depicted in the Figure 3.

The contact between the Ag coating of the wires and the metallization paste is small enough to be indistinguishable in the measure (Figure 4). The value obtained for the front grid resistance is $R_{s_{grid}} = 32{,}5 \pm 1{,}0\ m\Omega/cm$. During this measure, the current can also flow through the TCO even if its resistivity is several orders of magnitude higher. The resulting value is an equivalent resistance of finger and TCO.

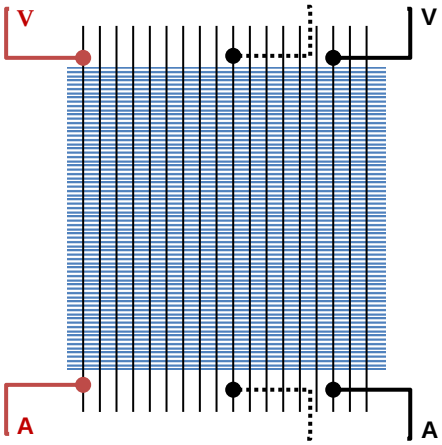

Figure 3: Measurement principle of the line resistance of the grid. Red probes are fixed to the first wire. Black probes are moved from one wire to another. The measurement is independent of the wire resistance.

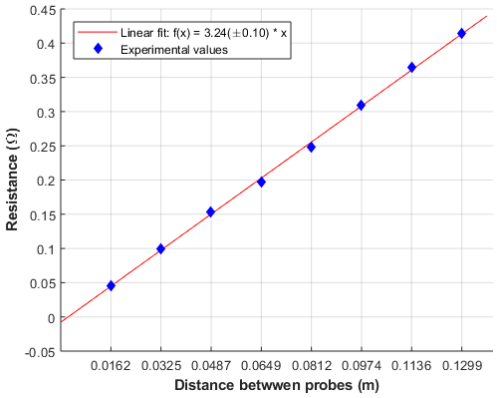

Figure 4: Measurement of the line resistance of the grid R_{line_g}. The deviation from linearity may be explained by the loss of contact between fingers and wires and the non-uniformity of the section of fingers.

3.2 Characterization of the absorption of the stack and effective diameter of the wires

The effective optical diameter of the module can be measured by varying the number of interconnecting wires, using the same cells, encapsulant and glass. The ratio of the photo-generated current of the module to the one of the cell has an affine dependency with the number of wires n_w. The y-axis intersection gives the value of k_{stack}, allowing to deduce the effective diameter from the slope of the curve:

$$\frac{I_{ph_{module}}}{I_{ph_c}} = \left(1 - {d_{eff}}_w \, n_w \left(L_w - n_f l_f\right) \frac{1}{A_c}\right) k_{stack}$$

Six mini-modules have been made, with 3, 6, 9, 12, 18, 24 wires of the same measured diameter of $d_w = 260 \pm 2\ \mu m$ and the results of the measure of their short circuit current is summarized in Table II.

From the linear fit of the curve in Figure 5, we get a value of $k_{stack} = 0.970 \pm 0.002$ and a value of effective diameter of $d_{eff} = 243 \pm 2\ \mu m$, with 95% confidence bounds. It corresponds to an effective wire shading equal to ${l_{eff}}_w = {d_{eff}}_w / d_w = 0.94 \pm 0.02$. This is different from the expected theoretical value of at least 0.75, mentioned in [4] and [7]. The theoretical effective shading should be around 0.7 when the cell is not encapsulated, due to the amount of light hitting the wire and directly reflected to the cell due to the round wire shape. When the cell is encapsulated, a portion of the impinging light is totally reflected at the air/glass interface while another portion is partially reflected. In this case, the effective shading can be as small as 0.35.

Table II: Cell and module short circuit currents for the six mini module made with varying number of wires.

n_w	$I_{sc_c}(A)$	$I_{sc_m}(A)$
3	9.320	9.001
6	9.243	8.892
9	9.262	8.873
12	9.283	8.837
18	9.292	8.764
24	9.251	8.657

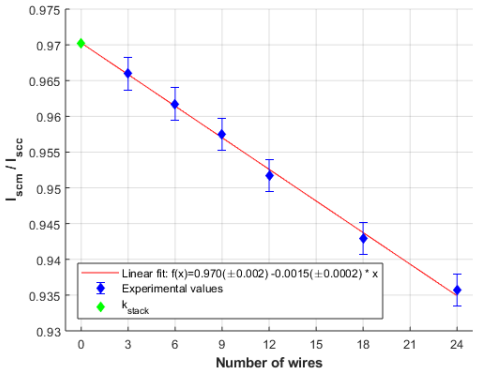

Figure 5: Short circuit current I_{sc} ratio between module and cell as a function of the number of wires n_w. The experimental values are the mean of three successive measurements, and the error is the standard deviation of the six modules.

No defects, such as trapped air around the encapsulated wires, could be seen via optical microscopy. Such defects could have explained the difference given the additional air/encapsulant interface. In the paper by McIntosh it is claimed that a small wire reflectance (R<0.5) can explain such a high value [8]. The difference in effective shading could be explained by the surface roughness of either the wire after melting and/or the glass. An increasing number of wires means also smaller coupling between cell and encapsulant, higher optical path of the incoming light in glass and encapsulant due to reflections. This different explanation needs further investigation.

4 RESULTS OF SENSITIVITY ANALYSIS

Resistivity of wires and string ribbons are determined with a good accuracy and the technological limit is almost reached: from a manufacturing stand point (wire production and handling during module manufacturing), it is difficult to decrease these values. On the other hand, there is a large range of possible values for effective shading of wires: from 35% to almost 100% as discussed in the previous part. Moreover, as the series resistance due

to fingers has a quadratic dependence on the number of wires, a small change in grid resistance can lead to huge changes in series resistance.

4.1 Reference case

The reference case is taken with the following parameters:

- Cells parameters as mentioned in 2.1
- Wire line resistance: 3.419 $m\Omega/cm$
- Distance inter-cell / inter-string: $3/5$ mm
- Measured grid resistance of 32.5 $m\Omega/cm$
- Measured effective shading of 94%
- Measured stack absorption of 97%

We investigate optimums in the range of 200 to 300 µm in core diameter, values commonly found in the industry. The results of the optimization are given in Figure 6. The optimum in CTM power is arbitrarily set at zero and we show contour lines from this reference level.

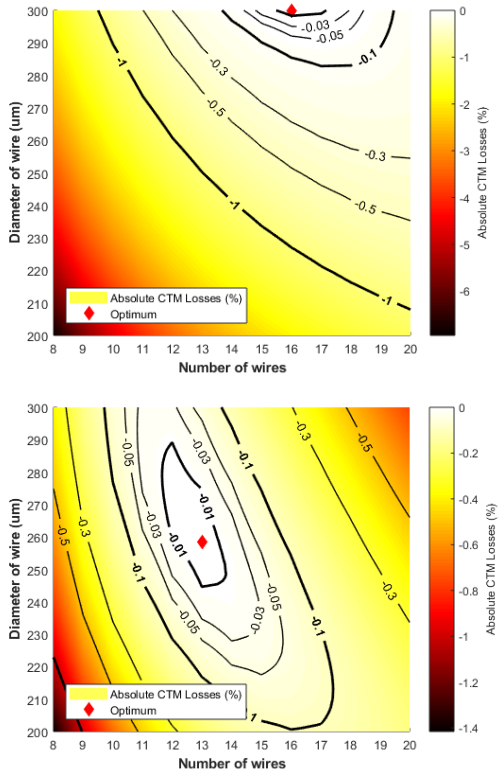

Figure 6: Absolute CTM Losses in percent compared to optimum case. The optimum is arbitrary put at zero level. Bold black contour lines are shown for 0.01%, 0.1% and 1% losses from optimum case. (Top) Full-cell design. The corresponding CTM_P of the optimal point is 91.3% (Bottom) Half-cell design. The corresponding CTM_P of the optimum is 93.5%.

The optimal number of wires in the full-cell case is 16 wires with a diameter of 300 µm. This optimum is found on the boundaries of the domain. This optimum corresponds to a CTM power of 91.3%. The optimal number of wires in the half-cell case is 19 with a diameter of 258 µm, corresponding to a CTM power of 93.5%. Going from full- to half-cell case presents a gain of 2.2%, which is the value expected [9]. Moreover, using half-cells decreases the volume of wires by 40% lower with respect to full-cells.

The optimal zone is flat, allowing choice flexibility, *e.g.* in the full-cell case (Figure 6, top graph), 9 wires with a 290 µm diameter produce the same level of losses than 20 wires with a diameter of 210 µm; *e.g.* fixing the diameter at 260 µm leads to an optimal wire number of 19.

4.2 Impact of grid resistance on optimal number and diameter of wires

In this part, we look at how the optimal number and diameter of wires varies when the grid resistance changes. All other parameters have been kept constant and particularly the cell resistance. Modifying the grid resistance without changing the cell series resistance is possible in two ways: changing either the shape factor of the finger, with an increasing height and a constant width, or the silver paste (with a different resistivity). The grid resistance of the reference case is 173 Ohm.cm²; a range between two times smaller and two times greater than this value is investigated.

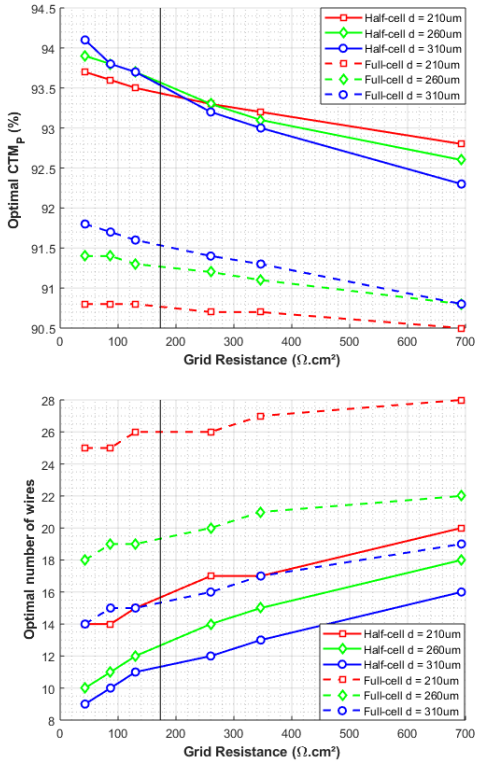

Figure 7: (Top) Results of the optimization in terms of CTM power for three diameters as a function of grid resistance. (Bottom) Corresponding optimal number of wires. Full-cell results are plotted in dashed line and half-cell in solid line. The vertical black line correspond to grid resistance value of the reference case in part 4.1

Results are shown in the Figure 7. The smaller the grid resistance, the greater the CTM power, with a corresponding optimal number of wires decreasing. The increase in CTM power is more pronounced for large wire diameters in both full- and half-cell case. The optimal number of wires is more dependent on the wire diameter in the full-cell case than in the half-cell one. Dividing the grid resistance by a factor two for halved-cells implies a gain in CTM of only +0.3% for diameter of 300 and 260 µm. However, the optimal number of wires falls from 13 (with 260 µm in diameter) to 11: this results in a possible decrease of the volume of wires of 15%.

4.3 Impact of effective shading on optimal number and diameter of wires

Effective shading ratio directly affects the photo-generated current and has a first order influence on power and CTM ratio. We consider the optimal number of wires varies and the CTM for three diameters. The effective shading ratio ranges from 40% to 100%.

Results are presented in Figure 8. Reducing the effective shading of the wires increases the CTM power and the optimal number of wires at the same time. The diameter of wires has almost no impact on the optimal CTM power in the half-cell case, as shown by the overlapping curves. However, the corresponding optimal number of wires is changing: 15 wires with a diameter of 200 µm for a 100% effective shading and 11 wires with a diameter of 300 µm. By reducing the effective shading ratio, the gain in CTM power is smaller in the half-cell case than in the full-cell case.

As the CTM gain is not affected by the wire diameter in half-cell, it is possible to choose the configuration of the lowest raw material consumption, *i.e.* 200 µm in diameter. Thus, going from the reference case in half-cell to a 50% effective shading with 200 µm (and thus 20 wires) implies same material consumption and a 1% gain in CTM power.

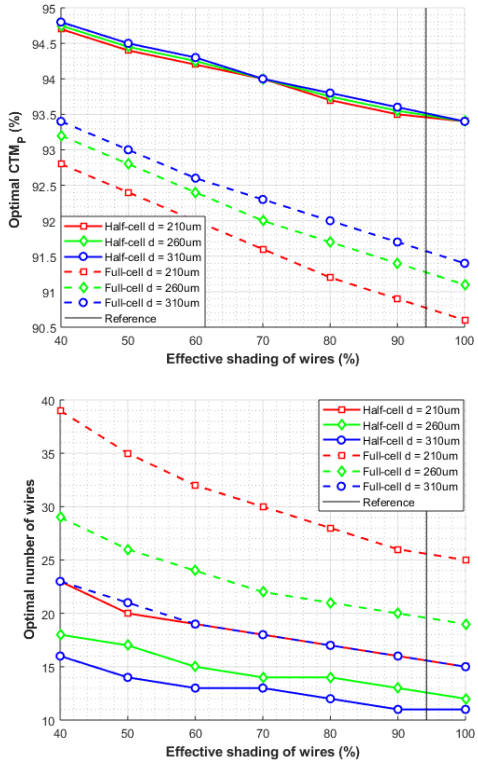

Figure 8: (Top) Results of the optimization in terms of CTM power for three diameters as a function of effective shading. (Bottom) Corresponding optimal number of wires. Full-cell results are plotted in dashed lines and half-cell in solid lines. The vertical black line corresponds to effective shading ratio of 94%, the reference case in part 4.1

5 CONCLUSION

A simple one-diode based model has been used to predict CTM ratio of a 72 equivalent hetorojunction Si-solar cell module with multi-wire interconnection technology. The number and the diameter of wires influences the series resistance and photo-generated current values in opposite ways, leading to an optimal value in CTM. We have studied how the optimum design in terms of number and diameter of wires is influenced by a change in grid resistance and effective shading of wires, in full-cell and half-cell architectures. Using half-cell allows to employ less wires with a smaller diameter than full-cell modules. As a result, both CTM performance and consumption of raw materials are improved.

Decreasing grid resistance, even if it allows using fewer wires, has only a small impact on CTM gain. On the other hand, the sensitivity analysis shows that effective shading value has a major impact on CTM, for constant raw material consumption. Thus, to make the optimization approach relevant, an accurate characterization of the effective shading of wires is needed.

As one of the major benefits of multi-wire interconnection is to reduce silver paste consumption, gain in the volume of wires should be balanced with volume of silver paste. The joint cost optimization should be considered as the next research advancement.

REFERENCES

[1] I. Haedrich, U. Eitner, M. Wiese, and H. Wirth, "Unified methodology for determining CTM ratios: Systematic prediction of module power," *Sol. Energy Mater. Sol. Cells*, vol. 131, pp. 14–23, Dec. 2014.

[2] J. Walter, M. Tranitz, M. Volk, C. Ebert, and U. Eitner, "Multi-wire Interconnection of Busbar-free Solar Cells," *Energy Procedia*, vol. 55, pp. 380–388, Jan. 2014.

[3] J. Roeth, A. Facchini, and N. Bernhard, "Optimized Size and Tab Width in Partial Solar Cell Modules including Shingled Designs," *International Journal of Photoenergy*, 2017. [Online]. Available: https://www.hindawi.com/journals/ijp/2017/3609109/. [Accessed: 17-Apr-2018].

[4] S. Braun, G. Hahn, R. Nissler, C. Pönisch, and D. Habermann, "The Multi-busbar Design: An Overview," *Energy Procedia*, vol. 43, pp. 86–92, Jan. 2013.

[5] "The GridTouch contacting system." 2014.

[7] J. Ufheil, P. Papet, and T. Söderström, "Smart Wire Connection Technology," *28th Eur. Photovolt. Sol. Energy Conf. Exhib.*, pp. 495–499, Nov. 2013.

[8] K. R. McIntosh, M. D. Abbott, M. B. Edwards, R. Evans, and Y. Yao, "Optical Evaluation of Multi-Wire Modules," *32nd Eur. Photovolt. Sol. Energy Conf. Exhib.*, pp. 15–19, Jul. 2016.

[9] S. Guo, J. P. Singh, I. M. Peters, A. G. Aberle, and T. M. Walsh, "A Quantitative Analysis of Photovoltaic Modules Using Halved Cells," *International Journal of Photoenergy*, 2013. [Online]. Available: https://www.hindawi.com/journals/ijp/2013/739374/. [Accessed: 25-May-2018].